

Resonance-like structure near the ηd threshold in the $\gamma d \rightarrow \pi^0 \eta d$ reaction

T. Ishikawa,^{1, a} H. Fujimura,^{1, b} H. Fukasawa,¹ R. Hashimoto,^{1, c} Q. He,^{1, d} Y. Honda,¹ T. Iwata,² S. Kaida,¹ J. Kasagi,¹ A. Kawano,³ S. Kuwasaki,¹ K. Maeda,⁴ S. Masumoto,⁵ M. Miyabe,¹ F. Miyahara,^{1, e} K. Mochizuki,¹ N. Muramatsu,¹ A. Nakamura,¹ K. Nawa,¹ Y. Obara,⁵ S. Ogushi,¹ Y. Okada,¹ K. Okamura,¹ Y. Onodera,¹ K. Ozawa,⁶ Y. Sakamoto,³ M. Sato,¹ H. Shimizu,¹ H. Sugai,^{1, f} K. Suzuki,^{1, g} Y. Tajima,² S. Takahashi,¹ Y. Taniguchi,¹ Y. Tsuchikawa,^{1, h} H. Yamazaki,^{1, i} R. Yamazaki,¹ and H.Y. Yoshida²

¹Research Center for Electron Photon Science (ELPH), Tohoku University, Sendai 982-0826, Japan

²Department of Physics, Yamagata University, Yamagata 990-8560, Japan

³Department of Information Science, Tohoku Gakuin University, Sendai 981-3193, Japan

⁴Department of Physics, Tohoku University, Sendai 980-8578, Japan

⁵Department of Physics, University of Tokyo, Tokyo 113-0033, Japan

⁶Institute of Particle and Nuclear Studies (IPNS),

High Energy Accelerator Research Organization (KEK), Tsukuba 305-0801, Japan

To investigate the interaction between the nucleon N and nucleon resonance $N(1535)1/2^-$, the ηd threshold structure connected to the isoscalar S -wave N - $N(1535)1/2^-$ system has been experimentally studied in the $\gamma d \rightarrow \pi^0 \eta d$ reaction at incident photon energies ranging from the reaction threshold to 1.15 GeV. A strong enhancement is observed near the ηd threshold over the three-body phase-space contribution in the ηd invariant-mass distribution. An analysis incorporating the known isovector resonance D_{12} with a spin-parity of 2^+ in the $\pi^0 d$ channel reveals the existence of a narrow isoscalar resonance-like structure with 1^- in the ηd system. Using a Flatté parametrization, the mass is found to be $2.427_{-0.006}^{+0.013}$ GeV, close to the ηd threshold, and the width is $(0.029_{-0.029}^{+0.006}$ GeV) + $(0.00_{-0.00}^{+0.41}) p_\eta c$, where p_η denotes the η momentum in the rest frame of the ηd system. The observed structure would be attributed to a predicted isoscalar $1^- \eta NN$ bound state from ηNN and πNN coupled-channel calculation, or an ηd virtual state owing to strong ηd attraction.

PACS numbers: 13.60.Le, 14.40.Be, 25.20.Lj

The structure and interaction of hadrons provides crucial insight into the non-perturbative mechanisms in quantum chromodynamics. Attraction between an η meson and a nucleon N makes it possible to form an η -mesic nucleus, as predicted by Haider and Liu [1]. This is an exotic state in which η is bound to the nucleus by the strong interaction force alone, and allows the study of the behavior of η in a dense nuclear environment. The binding energy of η in the nuclear medium is sensitive to a singlet component of η (η - η' mixing) [2–4]. The level and width of an η -mesic nucleus can yield the in-medium properties of nucleon resonance $N(1535)1/2^-$ (N^*) [5–8], which is speculated to be the chiral partner of N . This is because η in the nuclear medium is expressed by mixing of the η -mesonic state, and the N^* -particle and N -hole excitation state.

Exotic η -mesic nuclei have been intensively investigated theoretically, and searched for experimentally [9–11]. Experimental hints of possible η -mesic nuclei have been obtained in the threshold behavior of η -production reactions. The existence of an η -mesic nucleus enhances the cross section near the reaction threshold compared with phase space. The total cross section shows a steep increase from the threshold in $\eta^3\text{He}$ production from the pd collisions [12–14]. The possibility of an $\eta^3\text{He}$ weakly bound state is claimed by analyzing the η angular distribution [15]. If an $\eta^3\text{He}$ bound state exists, it should appear independently of the initial state of re-

actions. Coherent η photoproduction on ^3He also shows a strong threshold enhancement, and the angular distribution of η emission is rather flat near the threshold as compared with the expected distribution based on the nuclear form factor [16]. The WASA-at-COSY collaboration has searched for η -mesic ^3He and ^4He nuclei in the pd and dd reactions, respectively, by detecting daughter particles from η or N^* in a nucleus [17–21]. No convincing evidence for an η -mesic nucleus has yet been obtained.

An ηd bound state, if it exists, is the lightest η -mesic nucleus. The S -wave ηd system has an isospin of 0 and a spin-parity J^π of 1^- , and its properties are connected to the NN^* interaction. An ηNN bound state has been predicted near the ηd threshold with a width Γ of 0.01–0.02 GeV [22] from the three-body ηNN - πNN coupled-channel calculation. This state can be located lower than the threshold by 8 MeV [23]. This state is suggested by the significant deviation from phase space near the threshold in ηd production from the pn collisions [24–28]. In contrast, the $\gamma d \rightarrow \eta d$ reaction does not show any indication of this state; its angular distribution is explained by the quasi-free (QF) $\gamma N \rightarrow \eta N$ process [29, 30]. The possibility of an ηd bound state is ruled out in several theoretical three-body calculations for various ηN scattering parameters [31–33]. Instead, a narrow ηd virtual state is inferred to reproduce the experimental data [34–36]. However, qualitative disagreement is still observed in different theoretical calculations which cannot be ex-

plained by uncertainties in the ηN scattering parameters alone. It should be noted that the existence of an ηd bound or resonance state near the threshold is claimed in Ref. [37].

The $\gamma d \rightarrow \pi^0 \eta d$ reaction can provide a condition of low ηd relative momentum, producing a possible ηd bound state. In a similar $\gamma d \rightarrow \pi^0 \pi^0 d$ reaction, a sequential process $\gamma d \rightarrow \mathcal{D}_{\text{IS}} \rightarrow \pi^0 \mathcal{D}_{\text{IV}} \rightarrow \pi^0 \pi^0 d$ [38] is dominant, where \mathcal{D}_{IS} and \mathcal{D}_{IV} denote isoscalar and isovector states with a baryon number of 2, respectively. In $\gamma d \rightarrow \pi^0 \eta d$, the two sequential processes, $\gamma d \rightarrow \mathcal{D}_{\text{IV}} \rightarrow \pi^0 \mathcal{D}_{\text{IS}} \rightarrow \pi^0 \eta d$ and $\gamma d \rightarrow \mathcal{D}_{\text{IV}} \rightarrow \eta \mathcal{D}'_{\text{IV}} \rightarrow \pi^0 \eta d$, are expected to be observed, and the tail of the possible ηd bound state appears as \mathcal{D}_{IS} . In this letter, we study the $\gamma d \rightarrow \pi^0 \eta d$ reaction to clarify the structure that appears in the low-relative-momentum region of the ηd system generated after π^0 emission.

A series of experiments [39] were carried out using a bremsstrahlung photon beam [40–43] from 1.20-GeV electrons circulating in a synchrotron [44] at the Research Center for Electron Photon Science (ELPH), Tohoku University, Japan [45]. The photon energy ranging from 0.75 to 1.15 GeV was determined by detecting the post-bremsstrahlung electron with a photon-tagging counter, STB-Tagger II [40]. The target used was liquid deuterium with a thickness of 45.9 mm. All the final-state particles in the $\gamma d \rightarrow \pi^0 \eta d \rightarrow \gamma \gamma \gamma d$ reaction were measured with the FOREST detector consisting of three different electromagnetic calorimeters (EMCs) [46]. A plastic-scintillator hodoscope (PSH) was placed in front of each EMC to identify charged particles. The forward PSH could determine their impact positions. The trigger condition of the data acquisition required detection of multiple particles in coincidence with a photon-tagging signal [38, 46–48].

Initially, events containing four neutral particles and a charged particle were selected. An EMC cluster without a corresponding PSH hit was recognized as a neutral particle. A PSH hit gave a charged particle regardless of the existence of a corresponding EMC cluster. The time difference between every two neutral clusters out of four was required to be less than thrice that of the time resolution. The selected events were those in which the charged particle was detected with the forward PSH, under the conditions that the time delay from the response of the four neutral clusters was longer than 1 ns, and the deposit energy of a charged particle in PSH was greater than twice that of the minimum ionizing particle. Further selection was made by applying a kinematic fit (KF) with six constraints: energy and three-momentum conservation, the invariant mass of two photons out of four being the π^0 mass, and that of the other two being the η mass. The most probable combination was selected in each event for $\pi^0 \rightarrow \gamma \gamma$ and $\eta \rightarrow \gamma \gamma$. The momentum of the charged particle was obtained from the time delay assuming that the charged particle had the

deuteron mass. Events with χ^2 probability higher than 0.2 were selected to discriminate from other background reactions. The most competitive background was from deuteron misidentification events in the QF $\gamma p' \rightarrow \pi^0 \eta p$ reaction. Thus, selected events were additionally required to exhibit χ^2 probability below 0.01 in another KF for the $\gamma p' \rightarrow \pi^0 \eta p$ hypothesis where the x , y , and z momenta of the initial bound proton were assumed to be measured with a centroid of 0 MeV/ c and a resolution of 40 MeV/ c , and the total energy of the bound proton was given assuming the on-shell spectator neutron. Finally, sideband-background subtraction was performed for accidental-coincidence events detected in STB-Tagger II and FOREST.

The total cross section was obtained by estimating the acceptance of $\gamma \gamma \gamma d$ detection in a Monte Carlo simulation based on Geant4 [49–51]. Here, event generation was modified from pure phase space to reproduce the following three measured distributions: the $\pi^0 d$ invariant mass $M_{\pi d}$, the ηd invariant mass $M_{\eta d}$, and the deuteron emission angle $\cos \theta_d$ in the γd center-of-mass (CM) frame. Figure 1 shows the total cross section σ as a function of the incident photon energy E_γ (excitation function). The data obtained in this work were consistent with those ob-

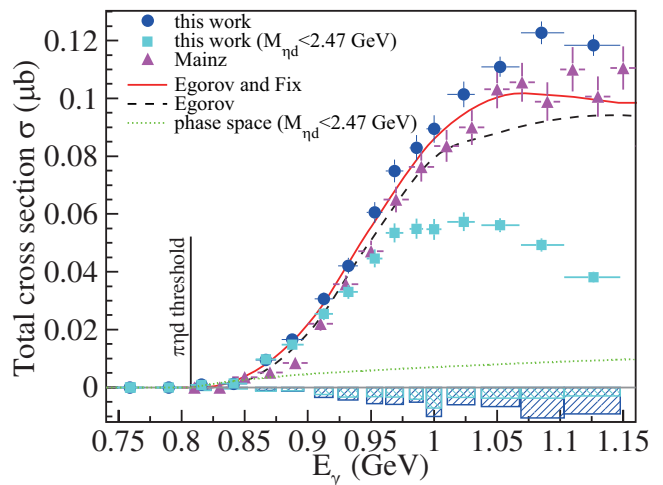


FIG. 1. Total cross section σ as a function of the incident photon energy E_γ . The circles (blue) show σ obtained in this work, and the triangles (magenta) show that obtained at the Mainz MAMI facility [52]. The horizontal error of each data point corresponds to the E_γ coverage, and the vertical error corresponds to the statistical error of σ . The solid (red) and dashed (black) curves show theoretical calculations with ηd and other FSIs in Ref. [53] and Ref. [54], respectively. The squares (cyan) show σ obtained for the events with $M_{\eta d} < 2.47$ GeV, and the dotted curve (green) shows the corresponding phase space contribution. The lower hatched histograms show the systematic errors of σ with right-up straight lines for all the events (blue) and with left-up lines for $M_{\eta d} < 2.47$ GeV (cyan).

tained at the Mainz MAMI facility [52]. The systematic uncertainty of σ is also given in Fig. 1. It includes the uncertainty of event selection in KF; that of acceptance owing to the uncertainties in the $M_{\pi d}$, $M_{\eta d}$, and $\cos\theta_d$ distributions in event generation of the simulation; that of deuteron detection efficiency; and that of normalization resulting from the numbers of target deuterons and incident photons. In Fig. 1, the data are compared with the existing theoretical calculations with the final-state interactions (FSIs) including ηd by Egorov and Fix [53] (red solid) and by Egorov [54] (black dashed). The excitation function is well-reproduced by these calculations near the threshold.

To study the ηd threshold structure, we obtained the differential cross section $d\sigma/dM_{\eta d}$ at $E_\gamma = 1.01\text{--}1.15$ and $0.95\text{--}1.01$ GeV as shown in Fig. 2 (left). The experimental data are presented by the circles with statistical errors, and the systematic uncertainties by the hatched histograms. An enhancement is observed in $d\sigma/dM_{\eta d}$ over the phase-space contribution (green dotted) in the low-mass region. This enhancement is much broader at $E_\gamma = 1.01\text{--}1.15$ GeV than at $E_\gamma = 0.95\text{--}1.01$ GeV, suggesting the appearance of another contribution from a resonance in the πd channel. We also obtained the differential cross section $d\sigma/dM_{\pi d}$ similarly to $d\sigma/dM_{\eta d}$ as shown in Fig. 2 (right). In $d\sigma/dM_{\pi d}$, we observe a significant enhancement at high masses, corresponding to the known isovector \mathcal{D}_{12} resonance with $J^\pi = 2^+$, $M \simeq 2.14$ GeV, and $\Gamma \simeq 0.09$ GeV [38].

Only the S -wave ηd system ($\mathcal{D}_{\eta d}$) forms a peak close to the threshold in $d\sigma/dM_{\eta d}$. The $\mathcal{D}_{\eta d}$ system with $J^\pi = 1^-$ decays into ηd dominantly in the S wave, and possibly in the D wave. The S - and D -wave contributions to the $d\sigma/dM_{\eta d}$ distribution differ in shape. A fraction of the D -wave contribution to the S -wave at a fixed $M_{\eta d}$ is proportional to p_η^4 , where p_η denotes the η momentum

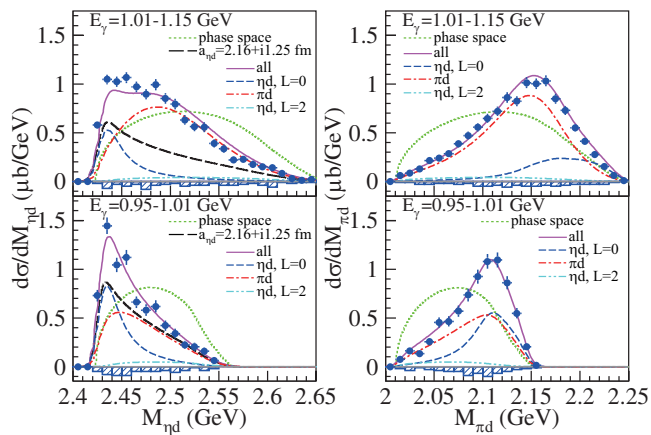


FIG. 2. Differential cross sections $d\sigma/dM_{\eta d}$ (left) and $d\sigma/dM_{\pi d}$ (right) at $E_\gamma = 1.01\text{--}1.15$ GeV (top) and $0.95\text{--}1.01$ GeV (bottom).

in the rest frame of the ηd system. The $\mathcal{D}_{\eta d}$ and \mathcal{D}_{12} contributions are separated by fitting a set of functions, expressed as the sum of S - and D -wave decay contributions of a Breit-Wigner (BW) resonance in the ηd channel and \mathcal{D}_{12} contribution in the $\pi^0 d$ channel, to the $M_{\eta d}$ and $M_{\pi d}$ data at $E_\gamma = 1.01\text{--}1.15$ and $0.95\text{--}1.01$ GeV simultaneously. The function for $d\sigma/dM_{\eta d}$ is given by

$$\frac{d\sigma}{dM_{\eta d}}(M_{\eta d}) = \alpha_0 \int A(M_{\eta d}, M_{\pi d}) V_{\text{PS}}(M_{\eta d}, M_{\pi d}) dM_{\pi d} \quad (1)$$

where $V_{\text{PS}}(M_{\eta d}, M_{\pi d})$ expresses the phase-space contribution and $A(M_{\eta d}, M_{\pi d})$ gives the enhancement owing to the two resonances:

$$A(M_{\eta d}, M_{\pi d}) = (1 + \alpha_2 p_\eta^4) L_{M,\Gamma}^{\mathcal{D}_{\eta d}}(M_{\eta d}) + \alpha_1 L_{M,\Gamma}^{\mathcal{D}_{12}}(M_{\pi d}). \quad (2)$$

Here, $L_{M,\Gamma}^{\mathcal{D}_{\eta d}}(M_{\eta d})$ and $L_{M,\Gamma}^{\mathcal{D}_{12}}(M_{\pi d})$ represent BW distributions with M and Γ for $\mathcal{D}_{\eta d}$ and \mathcal{D}_{12} , respectively. To incorporate the opening of the ηd channel, the ηd partial width is parametrized by the effective coupling g (known as the Flatté parametrization [60, 61]):

$$\Gamma = \Gamma_0 + gp_\eta c \quad (3)$$

for $\mathcal{D}_{\eta d}$, and Γ_0 is the width for the other open channels (NN , πNN , and $\pi\pi NN$). It should be noted that the phase space of the ηd decay is taken into account in $V_{\text{PS}}(M_{\eta d}, M_{\pi d})$. The other M and Γ parameters are assumed to be constant. Equation (1) is evaluated by the convolution of a Gaussian with an experimental mass resolution of $\sigma_{M_{\eta d}} = 6.0$ (4.8) MeV at $E_\gamma = 1.01\text{--}1.15$ (0.95–1.01) GeV. The function for $d\sigma/dM_{\pi d}$ is given by

$$\frac{d\sigma}{dM_{\pi d}}(M_{\pi d}) = \alpha_0 \int A(M_{\eta d}, M_{\pi d}) V_{\text{PS}}(M_{\eta d}, M_{\pi d}) dM_{\eta d} \quad (4)$$

with $\sigma_{M_{\pi d}} = 6.1$ (4.8) MeV at $E_\gamma = 1.01\text{--}1.15$ (0.95–1.01) GeV. In Fig. 2, the mass spectrum is an incoherent sum of two resonances for the following reason. As discussed later, we consider that $\mathcal{D}_{\eta d}$ and \mathcal{D}_{12} are produced in paths (5) and (6), respectively. The mass spectrum is a plot of the integrated yield for the angular distributions of π^0 and η . The interference term of the two paths is zero unless $L_1(\pi^0) = L_2(\pi^0)$ and $L_2(\eta) = L_1(\eta)$, owing to the orthogonality of the spherical harmonics which appear in the angular component of the wave function. In the analysis, the $L_1(\eta) = 1$ component is deduced to be $\sim 100\%$; therefore, almost no effect of the interference effect is expected in the mass spectra.

The obtained parameters in the fit are $(M, \Gamma_0, g) = (2.427_{-0.006}^{+0.006} \text{ GeV}, 0.029_{-0.029}^{+0.006} \text{ GeV}, 0.00_{-0.00}^{+0.41})$ for $\mathcal{D}_{\eta d}$, and $(M, \Gamma) = (2.158_{-0.003}^{+0.003}, 0.116_{-0.011}^{+0.005})$ GeV for \mathcal{D}_{12} , where $\chi^2 = 131.4$ and the number of data points is 76. Also plotted in Fig. 2 are the S - (blue dashed) and D -wave (cyan double-dotted) decay contributions as well as the \mathcal{D}_{12} contribution (red dot-dashed). Each of $d\sigma/dM_{\eta d}$

and $d\sigma/dM_{\pi d}$ consists of two peaks. The centroid of the low-mass peak in $d\sigma/dM_{\eta d}$ is close to the ηd threshold independently of E_γ . The high-mass peak reflects the appearance of the 2.14-GeV peak in $d\sigma/dM_{\pi d}$. The centroid of the high-mass peak decreases with a decrease of E_γ . Because the $M_{\pi d}$ coverage is limited at $E_\gamma = 0.95$ – 1.01 GeV, the two peaks merge into a bump in $d\sigma/dM_{\pi d}$ with substantial distortion of the 2.14-GeV peak. It is thus revealed that a narrow resonance-like structure exists in the vicinity of the ηd threshold (2.423 GeV). This is not observed due to its isoscalar nature in $\gamma d \rightarrow \eta d$ where the QF process is dominant.

The S -wave ηd resonance states with widths broader than 0.05 GeV are ruled out for the threshold enhancement in $d\sigma/dM_{\eta d}$. It could be attributed to the predicted ηd bound state [22, 23, 37], being a Feshbach resonance in the ηd and isoscalar πNN coupled channels. If so, the corresponding enhancement can be observed in the isoscalar πNN and $\pi^0\pi^0 d$ channels (corresponding to the $\Gamma_0 \neq 0$ case). Possibly related to this is a bump observed by the WASA-at-COSY collaboration at the CM energy of ~ 2.31 GeV in the isoscalar $NN \rightarrow \pi NN$ reaction [55]. The spin-parity of this bump is not clear (1^+ and 0^+ are discussed in Ref. [56, 57]), and the bump may include a 1^- state [58] corresponding to the ηd bound state.

The threshold enhancement can also be interpreted as an ηd virtual state [34–36] (corresponding to the $\Gamma_0 = 0$

case). The square of the amplitude would be proportional to $|a_{\eta d}^{-1} - ip_\eta|^{-2}$ for production of an ηd system at low relative momentum p_η , where $a_{\eta d}$ denotes the ηd scattering length. Using $a_{\eta d} = 2.16 + i1.25$ fm [59] extracted from $pn \rightarrow \eta d$ [27, 28], the $M_{\eta d}$ distributions are expected as shown by the long-dashed curves (black) in Fig. 2(left), and similar to the decomposed $\mathcal{D}_{\eta d}$ contributions close to the threshold. They are observed in a wider range as compared with the 10-MeV range of $pn \rightarrow \eta d$. High ηd angular momenta would be suppressed in $\gamma d \rightarrow \pi^0 \eta d$ because sequential processes are dominant. Additionally, the $pn \rightarrow \eta d$ data may be affected by FSI between η and the spectator proton.

The $\pi^0 \mathcal{D}_{\eta d}$ - and $\eta \mathcal{D}_{12}$ -produced processes are investigated using angular distributions of π^0 and η obtained for the events with $M_{\eta d} < 2.47$ GeV as shown in Fig. 3. Figure 3 (left) shows the deduced π^0 angular distributions in the γd -CM frame with respect to the incident photon direction; the experimental distributions are almost flat. The η angular distributions in the ηd rest frame with respect to the opposite direction to π^0 emission are shown in Fig. 3 (right). They take a convex-upward shape, and show almost 90° symmetry. Thus, contamination of a state with J^π other than 1^- (2^+) is assumed to be negligibly small in $\mathcal{D}_{\eta d}$ (\mathcal{D}_{12}).

We calculated the π^0 and η angular distributions for the reaction sequences of interest using the density matrix (statistical tensor) formalism [62]:

$$J_0(d) = 1 \xrightarrow{L_0(\gamma)} J_1(\pi^0 \mathcal{D}_{\eta d}) \xrightarrow{L_1(\pi^0)} J_2(\mathcal{D}_{\eta d}) = 1 \xrightarrow{L_2(\eta)=0,2} J_3(d) = 1 \quad (5)$$

and

$$J_0(d) = 1 \xrightarrow{L_0(\gamma)} J_1(\eta \mathcal{D}_{12}) \xrightarrow{L_1(\eta)} J_2(\mathcal{D}_{12}) = 2 \xrightarrow{L_2(\pi^0)=1} J_3(d) = 1, \quad (6)$$

where J_1 and J_2 denote the spins of first and second intermediate states, respectively, and $J_0 = J_3 = 1$ are those of the initial and final deuteron. The L_0 denotes the angular momentum of the incident photons. The L_1 and L_2 denote the angular momenta of meson emission from the first and second intermediate states, respectively. A set of the amplitudes $A_{\Lambda\Lambda'}$ was determined for all the $\Lambda = (L_0, J_1, L_1, J_2, L_2)$ combinations with $L_0, J_1, L_1 \leq 2$ to reproduce the measured angular distributions at $E_\gamma = 1.01$ – 1.15 and 0.95 – 1.01 GeV simultaneously (40 data points). The amplitude for a mixed state is given by $A_{\Lambda\Lambda'} = (A_{\Lambda\Lambda} A_{\Lambda'\Lambda'})^{1/2}$. The $L_2 = 2$ amplitudes are given by $A_{\Lambda_2\Lambda_2} = A_{\Lambda_0\Lambda_0} \tan \phi$, where $L_2 = 0$ in Λ_0 is replaced by $L_2 = 2$ in Λ_2 . The $L_2 = 1$ amplitudes are multiplied by an E_γ -dependent factor. The fractions of the $L_2 = 0, 1,$ and 2 contributions are limited

to 38.6%–49.3% (49.1%–57.5%), 50.0%–61.4% (41.3%–50.9%), and 0.0%–2.0% (0.0%–2.3%) for $E_\gamma = 1.01$ – 1.15 (0.95– 1.01) GeV, respectively, to match the results from the mass distribution analysis, giving a minimum χ^2 of 43.3. The solid curves (magenta) in Fig. 3 show the angular distributions calculated for the best-fit solution. The dashed (blue), dot-dashed (red), and two-dot-dashed (cyan) curves show the $L_2 = 0, 1,$ and 2 contributions, respectively. The long-dashed curves (black) represent the interference effects; those between even and odd L_2 s (between $L_2 = 0$ and 2) are observed in the π^0 (η) angular distributions. The $L_2 = 1$ amplitudes and the $L_2 = 0$ and 2 interference make the η angular distribution convex upward. Regarding $\pi^0 \mathcal{D}_{\eta d}$, the major component is 0^- ($\sim 47\%$), and the amplitudes are distributed widely to other 1^+ and 2^\pm components. For $\eta \mathcal{D}_{12}$, the major

component is 2^+ ($\sim 100\%$).

We also estimate the excitation function for the events with $M_{\eta d} < 2.47$ GeV, as represented by the squares (cyan) in Fig. 1. It forms a bump at ~ 1 GeV corresponding to the γd -CM energy of ~ 2.69 GeV. The observed broad bump corresponds to some resonances because the expected excitation function monotonically increases for the three-body phase-space contribution with $M_{\eta d} < 2.47$ GeV as plotted by the dotted curve (green) in Fig. 1. Loosely-coupled isovector S -wave molecules $N\Delta(1620)1/2^-$ and $N-N(1650)1/2^-$ would play the role of a doorway to the $\pi^0\mathcal{D}_{\eta d}$ system with 0^- . It should be noted that neither $\Delta(1620)1/2^-$ nor $N(1650)1/2^-$ is considered a contributor to the elementary $\gamma N \rightarrow \pi^0\eta N$ reaction (the main contributor is $\Delta(1700)3/2^-$) [63–67]. In contrast, $N-N(1720)3/2^+$ is a candidate doorway to $\eta\mathcal{D}_{12}$ with 2^+ although the branching ratio of $N(1720)3/2^+ \rightarrow \eta N$ is only a few percent [68].

In summary, the ηd threshold structure has been experimentally studied in the $\gamma d \rightarrow \pi^0\eta d$ reaction at $E_\gamma < 1.15$ GeV. It is found that the $M_{\eta d}$ dependence of $d\sigma/dM_{\eta d}$ is quite different from the behavior of the three-body phase space but shows a strong enhancement near the threshold, which changes in shape depending on the incident energy. An analysis incorporating the known resonance \mathcal{D}_{12} in the $\pi^0 d$ channel has revealed the existence of a narrow resonance-like structure in the S -wave ηd system, $\mathcal{D}_{\eta d}$. Applying a Flatté parameterization to $\mathcal{D}_{\eta d}$, we have obtained the mass of $2.427^{+0.013}_{-0.006}$ GeV and the width $\Gamma = \Gamma_0 + gp_\eta c$ with $\Gamma_0 = 0.029^{+0.006}_{-0.029}$ GeV and $g = 0.00^{+0.41}_{-0.00}$, where p_η denotes the η momentum in the ηd -CM frame, and g denotes the effective coupling to the

ηd channel. The S -wave resonance states with widths broader than 0.05 GeV are ruled out. The $\mathcal{D}_{\eta d}$ system would be the predicted ηd bound state, or an ηd virtual state originating from strong ηd attraction. The major component of the $\pi^0\mathcal{D}_{\eta d}$ system is found to be 0^- from the π^0 and η angular distributions for the events with $M_{\eta d} < 2.47$ GeV.

The authors express gratitude to the ELPH accelerator staff for stable operation of the accelerators in the FOREST experiments. They acknowledge Mr. Kazue Matsuda, Mr. Ken'ichi Nanbu, and Mr. Ikuro Nagasawa for their technical assistance in the FOREST experiments. They also thank Prof. Alexander I. Fix and Prof. Mikhail Egorov for their theoretical calculations and fruitful discussions. They are grateful for valuable discussions with Prof. Heinz A. Clement, Prof. Atsushi Hosaka, Prof. Kiyoshi Tanida, and Prof. Hiroyuki Fujioka. They acknowledge Prof. Bernd Krusche for the numerical values of the total cross sections measured at the Mainz MAMI facility. This work was supported in part by the Ministry of Education, Culture, Sports, Science and Technology, Japan (MEXT) and the Japan Society for the Promotion of Science (JSPS) through Grants-in-Aid for Specially Promoted Research No. 19002003, for Scientific Research (A) Nos. 24244022 and 16H02188, for Scientific Research (B) Nos. 17340063 and 19H01902, for Scientific Research (C) No. 26400287, and for Scientific Research on Innovative Areas Nos. 19H05141 and 19H05181.

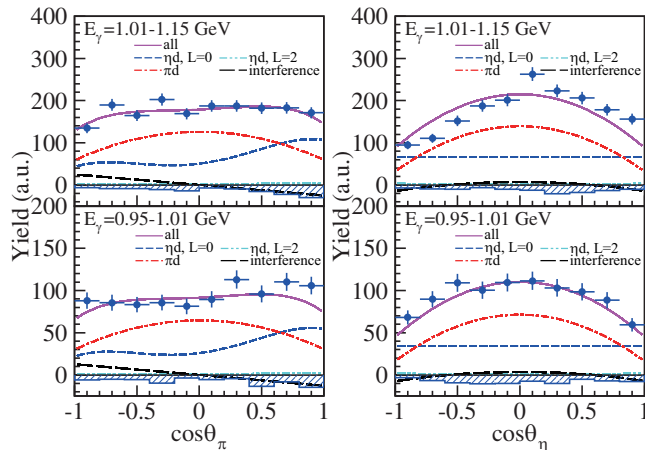


FIG. 3. Acceptance-corrected angular distributions for π^0 with respect to the photon beam direction in the γd -CM frame (left) and for η with respect to the opposite direction to π^0 in the ηd rest frame (right) at $E_\gamma = 1.01$ – 1.15 GeV (top) and 0.95 – 1.01 GeV (bottom). Events with $M_{\eta d} \leq 2.47$ GeV are selected.

- ^a Corresponding author: ishikawa@lns.tohoku.ac.jp
^b Present address: Department of Physics, Wakayama Medical University, Wakayama 641-8509, Japan
^c Present address: Institute of Materials Structure Science (IMSS), KEK, Tsukuba 305-0801, Japan
^d Present address: Department of Nuclear Science and Engineering, Nanjing University of Aeronautics and Astronautics (NUAA), Nanjing 210016, China
^e Present address: Accelerator Laboratory, KEK, Tsukuba 305-0801, Japan
^f Present address: Gunma University Initiative for Advanced Research (GIAR), Maebashi 371-8511, Japan
^g Present address: The Wakasa Wan Energy Research Center, Tsuruga 914-0192, Japan
^h Present address: J-PARC Center, Japan Atomic Energy Agency (JAEA), Tokai 319-1195, Japan
ⁱ Present address: Radiation Science Center, KEK, Tokai 319-1195, Japan
- [1] Q. Haider, and L.C. Liu, Phys. Lett. B **172**, 257 (1986).
[2] S.D. Bass, and A.W. Thomas, Phys. Lett. B **634**, 368 (2006).
[3] S. Hirenzaki, and H. Nagahiro, Acta Phys. Polon. B **45**, 619 (2014).
[4] S.D. Bass, and P. Moskal, Rev. Mod. Phys. **91**, 015003 (2019).
[5] D. Jido, H. Nagahiro, and S. Hirenzaki, Phys. Rev. C **66**, 045202 (2002).

- [6] H. Nagahiro, D. Jido, and S. Hirenzaki, *Phys. Rev. C* **68**, 035205 (2003).
- [7] H. Nagahiro, D. Jido, and S. Hirenzaki, *Nucl. Phys. A* **761**, 92 (2005).
- [8] D. Jido, E.E. Kolomeitsev, H. Nagahiro, and S. Hirenzaki, *Nucl. Phys. A* **811**, 158 (2008).
- [9] N.G. Kelkar, K.P. Khemchandani, N.J. Upadhyay, and B.K. Jain, *Rep. Prog. Phys.* **76**, 066301 (2013).
- [10] Q. Haider, and L.C. Liu, *Int. J. Mod. Phys. E* **24**, 1530009 (2015).
- [11] H. Machner, *J. Phys. G: Nucl. Part. Phys.* **42**, 043001 (2015).
- [12] B. Mayer *et al.*, *Phys. Rev. C* **53**, 2068 (1996).
- [13] J. Smyrski *et al.*, *Phys. Lett. B* **649**, 258 (2007).
- [14] T. Mersmann *et al.*, *Phys. Rev. Lett.* **98**, 242301 (2007).
- [15] J.-J. Xie *et al.*, *Phys. Rev. C* **95**, 015202 (2017).
- [16] B. Krusche, and C. Wilkin, *Prog. Part. Nucl. Phys.* **80**, 43 (2014).
- [17] P. Adlarson *et al.* (WASA-at-COSY collaboration), *Phys. Rev. C* **87**, 035204 (2013).
- [18] P. Adlarson *et al.* (WASA-at-COSY collaboration), *Nucl. Phys. A* **959**, 102 (2017).
- [19] M. Skurzok *et al.*, *Phys. Lett. B* **782**, 6 (2018).
- [20] P. Adlarson *et al.* (WASA-at-COSY collaboration), *Phys. Lett. B* **802**, 135205 (2020).
- [21] P. Adlarson *et al.* (WASA-at-COSY collaboration), *Phys. Rev. C* **102**, 044322 (2020).
- [22] T. Ueda, *Phys. Rev. Lett.* **66**, 297 (1991).
- [23] T. Ueda, *Phys. Lett. B* **291**, 228 (1992).
- [24] S.A. Rakityansky *et al.*, *Phys. Rev. C* **53**, 2043 (1996).
- [25] F. Plouin, P. Fleury, and C. Wilkin, *Phys. Rev. Lett.* **65**, 690 (1990).
- [26] H. Calén *et al.*, *Phys. Rev. Lett.* **79**, 2642 (1997).
- [27] H. Calén *et al.*, *Phys. Rev. Lett.* **80**, 2069 (1998).
- [28] R. Bilger *et al.*, *Phys. Rev. C* **69**, , (014003)2004.
- [29] P. Hoffmann-Rothe *et al.*, *Phys. Rev. Lett.* **78**, 4697 (1997).
- [30] J. Weißet *et al.*, *Eur. Phys. J. A* **11**, 371 (2001).
- [31] A. Deloff, *Phys. Rev. C* **61**, 024004 (2000).
- [32] H. Garcilazo and M.T. Peña, *Phys. Rev. C* **61**, 064010 (2000).
- [33] N. Barnea, E. Friedman, and A. Gal, *Phys. Lett. B* **747**, 345 (2015).
- [34] S. Wycech and A.M. Green, *Phys. Rev. C* **640452062001**.
- [35] A. Fix and H. Arenhövel, *Eur. Phys. J. A* **9**, 119 (2000).
- [36] H. Garcilazo, *Phys. Rev. C* **670670012003**.
- [37] N.V. Shevchenko *et al.*, *Eur. Phys. J. A* **9**, 143 (2000).
- [38] T. Ishikawa *et al.*, *Phys. Lett. B* **789**, 413 (2019).
- [39] T. Ishikawa *et al.*, *JPS Conf. Proc.* **10**, 031001 (2016).
- [40] T. Ishikawa *et al.*, *Nucl. Instrum. Meth. A* **622**, 1 (2010).
- [41] T. Ishikawa *et al.*, *Nucl. Instrum. Meth. A* **811**, 124 (2016).
- [42] Y. Matsumura *et al.*, *Nucl. Instrum. Meth. A* **902**, 103 (2018).
- [43] Y. Obara *et al.*, *Nucl. Instrum. Meth. A* **922**, 108 (2019).
- [44] F. Hinode *et al.*, in *Proceedings of 21st IEEE Particle Accelerator Conference (PAC)* (IEEE, Piscataway, 2005), pp. 2458–2460.
- [45] H. Hama, *AAPPS Bulletin* **30**, 41 (2020).
- [46] T. Ishikawa *et al.*, *Nucl. Instrum. Meth. A* **832**, 108 (2016).
- [47] T. Ishikawa *et al.*, *Phys. Lett. B* **772**, 398 (2017).
- [48] T. Ishikawa *et al.*, *Phys. Rev. C* **101**, 052201 (R) (2020).
- [49] S. Agostinelli *et al.*, *Nucl. Instrum. Meth. A* **506**, 250 (2003).
- [50] J. Allison *et al.*, *IEEE Trans. Nucl. Sci.* **53**, 270 (2006).
- [51] Geant4 website: (<http://geant4.cern.ch/>).
- [52] A. Käser *et al.*, *Phys. Lett. B* **748**, 244 (2015).
- [53] M. Egorov, and A. Fix, *Phys. Rev. C* **88**, 054611 (2013).
- [54] M. Egorov, *Phys. Rev. C* **101**, 065205 (2020).
- [55] P. Adlarson *et al.* (WASA-at-COSY collaboration), *Phys. Lett. B* **774**, 599 (2020); Corrigendum: *Phys. Lett. B* **806**, 135555 (2020).
- [56] V.I. Kukulini *et al.*, *Eur. Phys. J. A* **56**, 229 (2020).
- [57] H. Clement, and T. Skorodko, arXiv: 2010.09217 (2020).
- [58] H. Clement, private communication.
- [59] A. Fix, and O. Kolesnikov, *Phys. Rev. C* **97**, 044001 (2018).
- [60] S.M. Flatté, *Phys. Lett. B* **63**, 224 (1976).
- [61] Yu. S. Kalashnikova, and A.V. Nefedirev, *Phys. Rev. D* **80**, 074004 (2009).
- [62] L.C. Biedenharn, and M.E. Rose, *Rev. Mod. Phys.* **25**, 729 (1953).
- [63] M. Döring, E. Oset, and D. Strottman, *Phys. Rev. C* **73**, 045209 (2006).
- [64] J. Ajaka *et al.*, *Phys. Rev. Lett.* **100**, 052003 (2008).
- [65] A. Fix, V.L. Kashevarov, A. Lee, and M. Ostrick, *Phys. Rev. C* **82**, 035207 (2010).
- [66] V. Sokhoyan *et al.*, *Phys. Rev. C* **97**, 055212 (2018).
- [67] E. Gutz *et al.* (CBELSA/TAPS collaboration), *Eur. Phys. J. A* **50**, 74 (2014).
- [68] P.A. Zyla *et al.* (Particle Data Group), *Prog. Theor. Exp. Phys.* **2020**, 083C01 (2020).